https://doi.org/10.1016/j.colsurfa.2021.127490

Poly(allylamine)/Tripolyphosphate Coacervates for Encapsulation and Long-Term Release of Cetylpyridinium Chloride

Sabrina S. Alam,[1] Carolina B. Mather,[1] Youngwoo Seo,[1,2] Yakov Lapitsky[1,*]

[1] *Department of Chemical Engineering, University of Toledo, Toledo, Ohio 43606*

[2] *Department of Civil and Environmental Engineering, University of Toledo, Toledo, Ohio 43606*

* Corresponding author: Tel.: + 1-419-530-8254
Fax: + 1-419-530-8086

E-mail address: yakov.lapitsky@utoledo.edu

ABSTRACT: Complex coacervates formed through the association of poly(allylamine hydrochloride) (PAH) with pentavalent tripolyphosphate ions (TPP) have low solute permeabilities and enable multi-month release of small, water-soluble molecules. To this end, we have recently shown PAH/TPP coacervates to be highly effective in encapsulating and slowly releasing bioactive anionic surfactants. Here, we extend this work to the encapsulation and release of cationic surfactants and exploring the effects of the PAH/TPP/surfactant mixing order. Using cetylpyridinium chloride (CPC) as a model cationic amphiphile, we show that (like their anionic counterparts) cationic surfactants can be encapsulated in PAH/TPP coacervates in high concentrations (exceeding 20% of the coacervate weight). The high loadings evidently reflect the CPC/TPP association (which concentrates the CPC within the forming coacervates) and are maximized at high CPC concentrations, low PAH/TPP concentrations, and when the CPC is initially mixed with the TPP. This CPC encapsulation significantly affects the PAH/TPP coacervate properties (likely due to the considerable CPC/TPP association strength) and makes the coacervates opaquer and higher swelling, but less adhesive and less susceptible to spreading from their application sites. Besides increasing with their CPC content, the coacervate swelling varies with the PAH/TPP/CPC mixing order and is greatest when the CPC and TPP are mixed first. Once loaded, the CPC can be released over multiple months, with some control over the release rates (which, initially, are on the order of 10 μg/d, but tend to gradually fall below ~1 μg/d within the first 1 – 4 weeks). These findings suggest that PAH/TPP coacervates may be suitable for the low-dosage sustained release of cationic surfactants in applications where the release media has a low volume and is not frequently exchanged. More broadly, this work also indicates that: (1) effective encapsulation of active small molecules within polyelectrolyte/small multivalent counterion coacervates does not (when the payload associates with the small multivalent ions) require payload/polymer affinity; and (2) nonequilibrium effects during the formation of these payload-bearing coacervates can have long-term consequences on their properties and performance.

Keywords: Coacervate, Encapsulation, Sustained Release, Surfactant, Cetylpyridinium Chloride

https://doi.org/10.1016/j.colsurfa.2021.127490

1. INTRODUCTION

Complex coacervates are polymer-rich liquid phases that form through the complexation of polyelectrolytes with (typically oppositely charged) polymers [1-3], proteins [4, 5], surfactants [6, 7], or small multivalent ions [8-10]. These complex fluids have attracted broad interest in fields ranging from medicine and pharmaceutics [8, 11, 12], to food science [13], cosmetics [14-16], and bioseparations [17, 18]. Among the coacervate types that have been extensively studied is one composed of flexible primary polyamines, such as poly(allylamine hydrochloride) (PAH) or poly(L-lysine) (PLL), complexed with small multivalent anions [8, 19-25]. When these coacervates are prepared using more weakly associating multivalent counterions (e.g., citrate or phosphate), they easily flow from their application sites and have, thus, been primarily used as nanoscale thin films [23, 26] or (typically nanoparticle-stabilized) colloidal dispersions [8, 25, 27]. Conversely, when they are prepared using strongly associating multivalent counterions, such as pyrophosphate (PPi) or tripolyphosphate (TPP), these coacervates have more putty-like properties and can serve as either stimulus-responsive adhesives [21, 28] or as macroscopic ionic networks for highly sustained release [22, 29, 30].

When used for sustained release, these PAH/PPi and PAH/TPP networks, unlike typical hydrogels (where, in the absence of payload-network affinity, small molecule diffusion is rapid [31]), provide effective diffusion barriers and enable the release of small molecules over multiple months [22, 29, 30]. Such sustained release could make these materials attractive for diverse controlled release applications, ranging from drug delivery to household disinfection or fragrance release. Recently, using the weakly amphiphilic drug, ibuprofen (critical micelle concentration, CMC = 180 mM [32]) as a model payload, our lab has shown that PAH/TPP coacervates may be

https://doi.org/10.1016/j.colsurfa.2021.127490

particularly effective in achieving very high loading and multi-month release of weak anionic surfactants [30].

Ibuprofen was first (through simple mixing) allowed to form colloidal complexes with the PAH, whereupon TPP was added. Because PAH/TPP binding was stronger than PAH/ibuprofen binding, the PAH/ibuprofen complexes were transformed into PAH/TPP coacervates. Since ibuprofen was localized around the PAH chains, however, it ended up being concentrated inside the coacervates, producing PAH/TPP networks containing up to roughly 30 wt% ibuprofen [30]. Despite these high loadings, the PAH/TPP coacervates largely preserved their properties and were able to release the ibuprofen over more than 6 months. When the weakly amphiphilic ibuprofen was replaced with stronger sodium dodecylbenzene sulfonate (SDS; CMC = 8 mM [33]) and sodium dodecylbenzene sulfate (SDBS; CMC = 3 mM [34]) surfactants, however, the competitive surfactant association with PAH significantly changed the coacervate optical and rheological properties and increased the coacervate permeability to small molecule solutes [30].

Here, building on these prior efforts, we explore whether PAH/TPP coacervates might produce similar effects with the encapsulation of cationic surfactants, which find broad use in home and personal care products and can serve as disinfectants [35-37], through the association of cationic surfactants with TPP. Cetylpyridinium chloride (CPC; CMC ≈ 1 mM [38]), which serves as an antibacterial and antiviral agent [39, 40] in various applications — including oral care [41-43], cosmetic, and fabric care formulations [44-46] — is used as a model cationic molecule. CPC/TPP association is first examined through potentiometric titrations and phase studies. UV-vis spectroscopy and gravimetry are then used to examine the impact of CPC addition on PAH/TPP coacervation and characterize the CPC uptake performance. Unlike the previous studies on PAH/TPP coacervates, where each model payload was encapsulated through a single mixing

https://doi.org/10.1016/j.colsurfa.2021.127490

method [22, 29, 30], these coacervation/uptake analyses also probed the influence of the mixing procedure (i.e., of whether the CPC was initially mixed with the PAH or the TPP). To gain insights into the PAH/TPP coacervate stability, the effects of CPC encapsulation and the presence of various salts on the PAH/TPP coacervate swelling were also explored. Finally, the impacts of various process and formulation parameters on the CPC release rates were characterized.

2. MATERIALS AND METHODS

2.1. Materials

Deionized water (18.2 MΩ·cm resistivity) which, unless otherwise stated, was used for all experiments, was obtained from a Millipore Direct-Q water purification system. TPP (sodium salt), cetylpyridinium chloride (CPC), and ninhydrin reagent (2,2-dihydroxyindane-1,3-dione) for PAH quantification, and Rhodamine B (RhB) were purchased from Sigma-Aldrich (St. Louis, MO). PAH (nominal molecular weight = 150 kDa; 40 wt% solution) was obtained from Nittobo Co. (Tokyo, Japan). Ethanol and hydrochloric acid (HCl) were purchased from Fisher Scientific (Fair Lawn, NJ) and sodium hydroxide (NaOH) was bought from VWR (West Chester, PA). All materials were used as received.

2.2. Analysis of CPC/TPP Interactions

CPC interactions with PAH and TPP were qualitatively characterized via potentiometric titration. The CPC/TPP complexes were prepared at a 0.20:1 CPC:TPP molar ratio (i.e., 1:1 charge ratio when TPP is fully ionized) by mixing a 68 mM CPC solution (pH 7.0) with a pH-matched, 14 mM TPP solution. To prepare the CPC/TPP mixture for the titration, its pH was then lowered to 2.0 using HCl, whereupon it was titrated with 20-μL aliquots of 6 M NaOH (recording the pH

https://doi.org/10.1016/j.colsurfa.2021.127490

after each addition) until the measured pH exceeded 12. As controls, similar acid-base titrations were also conducted on TPP-free 68 mM CPC solutions and CPC-free 14 mM TPP solutions. Likewise, to probe PAH/CPC interactions, these titrations were performed on aqueous mixtures of CPC and PAH (68 mM of each) and, as a control, CPC-free 68 mM PAH solutions.

To further characterize the CPC/TPP interactions, a phase map was generated by preparing CPC/TPP mixtures at different compositions, equilibrating them at 25 ℃ and visually observing them over 3 months. The CPC and TPP solutions were warmed to 25 ℃ by placing them in a water bath for 1 h before mixing. The CPC/TPP mixtures were then prepared by equivolumetric mixing of variably concentrated CPC and TPP solutions in glass test tubes.

2.3. Preparation of CPC-Loaded Coacervates

CPC-loaded PAH/TPP coacervates were produced by adding CPC to the PAH and/or TPP solutions used in their preparation. To generate CPC-bearing parent PAH solutions, 5 mL of 2 – 20 wt% (56 – 560 mM) aqueous CPC solution was prepared and then mixed with an equal volume of 2 – 20 wt% (0.24 – 2.4 M in its monomer units) PAH solutions. To ensure thorough mixing, the CPC-bearing PAH solutions were vortexed for roughly 10 s and stirred for 6 h at 200 rpm with a 12 mm × 4 mm cylindrical magnetic stir bar. The solutions were then equilibrated for 24 h in a 30 °C water bath. To prepare CPC-bearing TPP parent solutions, 10 mL of 1.9 − 7.5 wt% (53 − 220 mM) TPP solution containing 28 – 140 mM CPC were prepared by adding CPC to premade TPP solutions. These solutions were mixed, vortexed, and then stirred at 200 rpm for 2 h with a magnetic stir bar, and equilibrated for 10 h in a 30 °C water bath. Conversely, to prepare CPC-free PAH and TPP solutions, 2.5 – 10 wt% PAH (0.29 – 1.2 M) solutions and 1.9 – 7.5 wt% (21 – 220

https://doi.org/10.1016/j.colsurfa.2021.127490

mM) TPP solutions were prepared. All solutions were then adjusted to pH 7.0 with either NaOH or HCl.

To form CPC-loaded coacervates, the PAH and TPP solutions (at least one of which contained CPC) were mixed inside centrifuge tubes. When CPC-bearing TPP solutions were used, 0.75 − 3.0 mL of 2.5 − 10 wt% (0.29 − 1.2 M) PAH solution was placed into either 2 or 15 mL centrifuge tubes, after which 0.8 − 3.2 mL of CPC-bearing 1.9 − 7.5 wt% (53 − 220 mM) TPP solution (containing 28 – 140 mM CPC) was added all at once. For CPC-bearing PAH solutions (also containing 28 – 140 mM CPC), on the other hand, 0.8 − 3.2 mL of CPC-free 1.9 − 7.5 wt% (53 − 220 mM) TPP solution was placed into the centrifuge tubes, whereupon 0.75 − 3.0 mL aliquots of CPC-loaded 2.5 − 10 wt% (0.29 − 1.2 M) PAH solution were added. Further, in some experiments (vide infra), CPC was added to both of the (PAH and TPP) solutions used in the coacervation process. The TPP:PAH molar ratio was kept constant at 0.20:1, while the solution volumes (e.g., 0.75 mL of 10 wt% PAH solution versus 3 mL of 2.5 wt% PAH solution) were varied to contain identical PAH and TPP amounts (and thus produce similar coacervate volumes).

2.4. Ninhydrin Analysis of PAH/TPP Coacervation

Because PAH/TPP association depends strongly on the TPP:PAH molar ratio, pH, ionic strength, and presence of competitively binding molecules [21], we examined the impact of CPC on PAH/TPP complexation efficiency. This analysis was performed by quantifying the free PAH content remaining in the supernatant phase upon coacervation using the ninhydrin assay [29, 47]. CPC-free coacervates and coacervates formed with 14 – 72 mM CPC (mixed into either the parent PAH solution or the parent TPP solutions) were analyzed. To quantify free PAH in the supernatant, 0.5 mL supernatant samples were mixed with 0.5 mL of ninhydrin reagent in 6 mL glass test tubes,

https://doi.org/10.1016/j.colsurfa.2021.127490

whereupon the tubes were immediately capped. The tubes were then shaken and heated in boiling water for 30 min, after which the tubes were cooled to 25 ºC using a water bath. After cooling the test tubes to 25 ºC by placing them in a water bath for 10 min, 2.5 mL of 50 vol% ethanol/water mixture was added to each tube. The solutions (and similarly treated deionized water controls) were then vortexed for 30 s and analyzed for their PAH content by UV-vis spectroscopy (λ = 570 nm, ε = 52.1 mL mg^{-1} cm^{-1}), using a Cary 50 UV-vis spectrometer (Sparta, NJ). Coacervate yields at different CPC concentrations were determined (by analyzing three replicate samples) as [29]:

$$\%Yield = \left(\frac{C_i - C_s}{C_i} \right) \times 100\% \quad (1)$$

where C_i was the initial/overall PAH concentration obtained upon PAH/TPP mixing, while C_s was the free PAH concentration ultimately remaining in the supernatant.

2.5. CPC Uptake Analysis

CPC-loaded coacervates were prepared as described in Section 2.3 and, upon their centrifugation into pellets, the supernatant phases were separated and analyzed by UV-vis spectroscopy (at λ = 260 nm, ε = 12 mL mg^{-1} cm^{-1}). The CPC loading capacity (LC) and loading efficiency (LE) within the PAH/TPP coacervates were then quantified as:

$$LC = \left(\frac{V_t C_i - V_s C_s}{W_0} \right) \times 100\% \quad (2)$$

$$LE = \left(\frac{V_t C_i - V_s C_s}{V_t C_i} \right) \times 100\% \quad (3)$$

where C_i was the initial/overall CPC concentration in the mixture, C_s was the molar CPC concentration remaining in the supernatant, V_s was the supernatant volume, V_t was the total mixture

https://doi.org/10.1016/j.colsurfa.2021.127490

volume, and W_0 was the initial coacervate weight upon the removal of the supernatant phase. These experiments were reproduced three times for each coacervate composition.

2.6. Gravimetric Analysis of Coacervate Swelling

Gravimetric analyses were performed on the CPC-loaded PAH/TPP coacervates to characterize their swelling and stability in tap water (pH 9.6 ± 0.5; turbidity ≈ 0.2 – 0.4 NTU). To measure the initial CPC-loaded coacervate weight, the supernatant was discarded from the centrifuge tubes, using Kimwipe™ tissues to remove any excess solution remaining on the coacervate surface. The coacervates were then submerged in 1 mL of tap water and shaken in an Eppendorf Thermomixer (Hamburg, Germany) at 600 rpm and room temperature (20 – 25 ºC). The tap water swelling/release medium was changed daily for the first 4 d and every other day for another 8 d. Then, for another 32 d, the medium was changed every 4 d and, at longer times, where the amounts of CPC released over 4 d diminished below its detection limit (as these samples were also used to measure CPC release), the release medium was replaced every 10 d. To probe the CPC-loaded coacervate swelling/stability, the wet coacervate weights were measured whenever the release medium was changed. These weights were then normalized to the initial values as $W(t)/W_0$, where $W(t)$ was the coacervate weight at the time, t, and W_0 was the weight prior to its placement in tap water.

To also better understand the effect of salt addition on the swelling/stability of CPC-loaded PAH/TPP coacervates in the presence of some common ions they may encounter during use, coacervates were prepared from 10 wt% (1.2 M) PAH and 7.5 wt% (220 mM) TPP parent solutions (with the PAH solutions containing 84 mM CPC). The supernatant phases were then discarded, and the microcentrifuge tubes were filled with 1 mL of either 10 mM $CaCl_2$ solution, 10 mM NaCl

https://doi.org/10.1016/j.colsurfa.2021.127490

solution, or 10 mM Na_2SO_4 solution. The microcentrifuge tubes were then agitated at room temperature as described previously. The salt solutions were replaced every other day and the coacervate weights were recorded. Three replicate samples were used for all swelling experiments.

2.7. CPC Effect on PAH/TPP Coacervate Spreading

To qualitatively probe the effect of CPC uptake and parent PAH solution concentration on the resistance of CPC-loaded PAH/TPP coacervates to spreading from their application sites, both control coacervates (without CPC) and CPC-loaded coacervates were prepared as described previously (by adding 56 mM CPC to both of the parent PAH/TPP solutions). Coacervate samples (0.16 – 0.17 g) were then placed at the centers of polystyrene Petri dishes (Ø = 83 mm), whereupon 4-mL portions of the supernatant phases obtained during coacervation were added to keep the coacervates hydrated. The Petri dishes were then covered, sealed with Parafilm, and monitored for changes in coacervate diameters over 7.5 d, with each experiment repeated in triplicate.

2.8. CPC Release Studies

CPC release from PAH/TPP coacervates was analyzed by measuring the CPC concentration in the release medium by UV-vis spectroscopy (at $\lambda = 260$ nm, $\varepsilon = 12$ mL mg^{-1} cm^{-1}). To model the release of an antibacterial cationic surfactant for household applications, room-temperature (20 – 25 ºC) tap water was chosen as the release medium. The coacervates, which remained in the microcentrifuge tubes used in their preparation (see Section 2.3), were covered with 1 mL of tap water (pH 9.6 ± 0.5 and turbidity ≈ 0.2 – 0.4 NTU) and, to limit CPC accumulation in the release medium, this tap water was periodically replaced (as described in Section 2.6). Further, to assess the release medium volume effects on CPC release, several release experiments

https://doi.org/10.1016/j.colsurfa.2021.127490

were repeated using a higher, 10-mL release medium volume. These modified experiments were performed as described above, except the coacervate-bearing microcentrifuge tubes (Ø = 11 mm) were stripped of their caps and submerged in 10 mL of tap water inside larger, 15-mL Falcon™ centrifuge tubes (Ø = 17 mm). In each case, CPC release was measured by analyzing the released CPC content in tap water each time that the tap water release medium was replaced. The release from each coacervate sample was monitored until the CPC concentration in the release medium became too low to detect with the UV-vis spectrophotometer after allowing CPC to accumulate in the release medium for 10 d. Three replicates were analyzed for each experimental condition.

3. RESULTS AND DISCUSSION

3.1. Analysis of CPC/TPP Interactions

Visual observation of CPC/TPP mixtures revealed that CPC/TPP association led to phase separation over a broad range of conditions (see Fig. 1). This associative phase separation was sensitive to the CPC and TPP concentrations. At lower concentrations, the CPC/TPP complexes formed flaky precipitates (P), which coexisted with dilute supernatant (S) phases. At higher concentrations, however, the CPC/TPP association was weakened (i.e., self-screened) by the higher concentrations of released monovalent (Na^+ and Cl^-) counterions [30, 48]. Thus, as the CPC and TPP concentrations were raised, the CPC/TPP precipitates first turned into less tightly associated liquid coacervates (C), then into less highly aggregated colloidal dispersions (D) and, finally, in the limits of very high CPC and TPP concentrations, were fully dissolved (Fig. 1). Similarly, single-phase mixtures were obtained in highly nonstoichiometric CPC/TPP mixtures, which formed complexes that were either highly charged or screened enough to remain soluble [49]. These solutions generally formed when the CPC surfactant concentration exceeded the

https://doi.org/10.1016/j.colsurfa.2021.127490

charge equivalence line (dashed line in Fig. 1, indicating the 0.2:1 pentavalent TPP anion:CPC cation ratio), and when the TPP concentration was raised beyond 20 – 50 mM. These phase behavior trends confirmed the presence of CPC/TPP binding, which was qualitatively consistent with prior work, where phosphate-mediated removal of CPC from water revealed a similar association between CPC and phosphate ions [50].

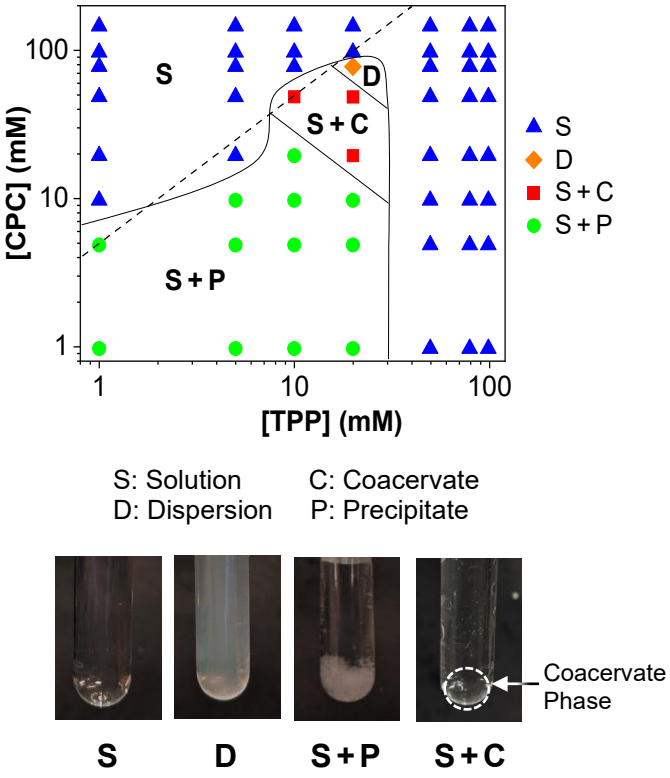

Fig. 1. Phase map of CPC/TPP mixtures indicating compositions where single-phase solutions, stable colloidal dispersions, macroscopic flaky precipitates, and macroscopically separated complex coacervates form. The macroscopic coacervates (C) and precipitates (P) coexist with supernatant solution phases (S), while the dispersions (D) remain in a single macroscopic phase. The dashed line represents stoichiometric CPC:TPP charge ratios, calculated under the assumption of TPP being fully ionized. All samples were equilibrated for 3 months at 25 °C.

Further insight into CPC/TPP association came from potentiometric titration experiments, where acid-base titrations of CPC and TPP solutions, and their 1:1 charge ratio mixtures (estimated

https://doi.org/10.1016/j.colsurfa.2021.127490

based on the charge of fully ionized TPP) were performed. In the acid-base titration of the TPP solution, there was strong buffering over a wide spectrum of pH-values, which (particularly between pH 4 and 11) was evident from the gradual rise in pH with the NaOH addition (circles in Fig. 2). This buffering stemmed from TPP ($pK_{a,3}$ = 2.8, $pK_{a,4}$ = 6.5, and $pK_{a,5}$ = 9.2) being a polyprotic acid with multiple pK_a-values [51]. Conversely, because CPC was a strong cation, it did not act as a buffer, and the pH rose sharply (especially when it was in the 3 – 11 range) with the addition of NaOH (triangles in Fig. 2). Further, when TPP and CPC were mixed, the buffering seen in the TPP solution was drastically weakened (squares in Fig. 2). Thus, in CPC/TPP mixtures, fewer ionizable TPP groups were free to be protonated or deprotonated with the changes in pH. This indicated that TPP/CPC binding was stable in this pH range (i.e., that this binding was quite strong).

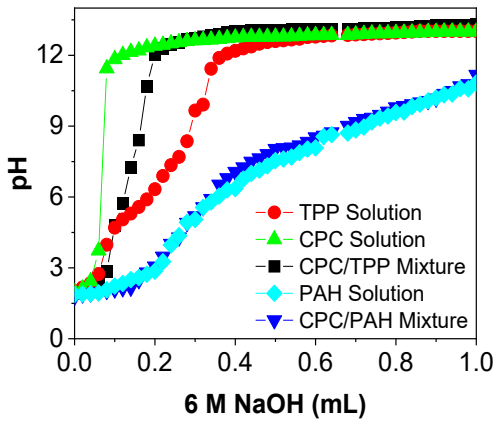

Fig. 2. Acid-base titration curves for a TPP solution, a CPC solution, a CPC/TPP mixture with a 0.2:1 TPP:CPC molar ratio, a PAH solution, and a CPC/PAH mixture with a 1:1 PAH:CPC molar ratio. The CPC, PAH, and TPP concentrations are 68, 68, and 14 mM, respectively (where the PAH concentration is the monomer unit concentration). The lines are guides to the eye.

When CPC was mixed with PAH, on the other hand, it (since both species were cationic) did not strongly interact with the ionizable amine groups on the PAH. Thus, the acid-base titration curves for the equimolar PAH/CPC mixture nearly overlapped the titration curve obtained for the

https://doi.org/10.1016/j.colsurfa.2021.127490

CPC-free PAH solution (inverted triangles and diamonds in Fig. 2). The effective pK_a value of PAH is near 8.7 [52] and, in both cases, buffering by the PAH — as is characteristic of polyelectrolytes [52, 53] — occurred over a broad range of pH values. Overall, these titrations suggested that the addition of CPC could inhibit coacervation due to its strong association with TPP (which could reduce PAH/TPP crosslinking) but should not limit the availability of PAH amine groups.

3.2. Compositional Effects on the Coacervate Yield

Mixing of PAH with CPC/TPP mixtures or TPP with CPC/PAH mixtures produced macroscopic PAH/TPP coacervates that encapsulated CPC. These CPC-loaded coacervates were more opaque than their CPC-free counterparts (see inset in Fig. 3a) and, despite still being tacky, (in contrast to the CPC-free coacervates) detached from the microcentrifuge tube wall surface upon vortex mixing. This qualitative change in coacervate properties was akin to that reported upon the encapsulation of strong anionic surfactants (SDS and SDBS, whose CMCs were comparable to that of CPC), which were associated with PAH and suggested possible persistence of CPC/TPP binding within the coacervate phase [30]. Due to this competitive CPC/TPP binding, PAH/TPP association was generally impeded by CPC, and the coacervate yield (which was estimated based on the percentage of PAH in the coacervate phase) slightly decreased with CPC addition. As the CPC concentration in the final PAH/TPP/CPC mixture increased from 0 to 68 mM (and the CPC:TPP molar ratio increased from 0.00 to 0.62:1), the PAH yield decreased by 3 – 4%, which might have reflected an increase in competitive CPC/TPP complexation (Fig. 3a). This reduction in PAH coacervation, however, was very modest. The reasons for this limited effect could be twofold: (1) the concentration of PAH amine groups in the PAH/TPP/CPC mixture (570 mM) was

https://doi.org/10.1016/j.colsurfa.2021.127490

much higher than that of the CPC; and (2) PAH/TPP affinity may have, like in the ibuprofen encapsulation study [30], exceeded that of TPP association with CPC. The latter of these effects might have reflected the PAH having primary amine groups, whose binding to multivalent anions has been reported to be stronger than that of the quaternary amine groups on the CPC [54, 55].

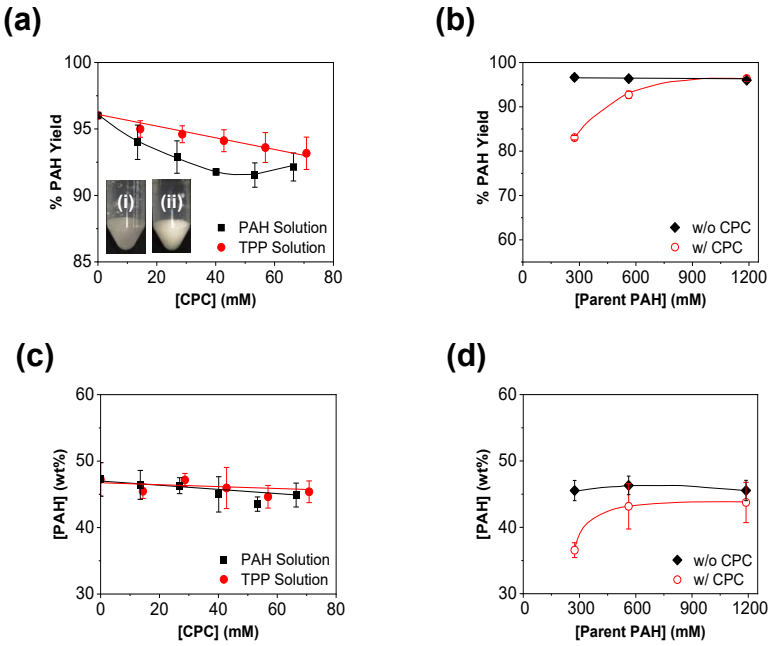

Fig. 3. Variations in (a, b) coacervate yields and (c, d) PAH concentrations within the coacervates as functions of (a, c) overall CPC concentrations achieved by initially adding the CPC to either the parent PAH or the parent TPP solutions, and (b, d) parent PAH solution concentrations, where the coacervates were formed either in the absence of CPC or in the presence of 25 mM CPC. All samples in (a, c) were prepared using 10 wt% (1.2 M) PAH and 7.5 wt% (220 mM) parent TPP solutions, while those in (b, d) were prepared using 2.5 – 10 wt% PAH (0.29 − 1.2 M) and 1.9 – 7.5 wt% TPP (53 − 220 mM) solutions (both containing 25 mM CPC). The TPP:PAH molar ratio in all final mixtures was fixed at 0.20:1. The insets in plot (a) are representative images of coacervates (i) without and (ii) with CPC. All data are mean ± SD, while the lines are guides to the eye.

Interestingly, the coacervate yield also depended on whether CPC was initially added to the parent PAH solution or the parent TPP solution (before the PAH/TPP mixing). Though in both cases PAH yield slightly decreased with the CPC concentration, this effect was always somewhat stronger when the CPC was initially added to the PAH solution (Fig. 3a). These mixing-process

https://doi.org/10.1016/j.colsurfa.2021.127490

dependent differences in yield suggested the coacervates that form upon CPC encapsulation to be nonequilibrium systems whose compositions and properties are kinetically controlled.

Another minor determinant of PAH yield was the parent PAH solution concentration. As the PAH concentration was increased from 2.5 to 10 wt% (from 0.29 to 1.2 M) in the absence of CPC, the PAH yield slightly decreased (by 0.7%; see Fig. 3b). When the experiment was repeated in the presence of 25 mM CPC, however (which was added to both of the parent PAH/TPP solutions), this trend was reversed, and the PAH yield increased with the parent PAH solution concentration. This increase likely reflected the enhanced ability of the more concentrated PAH to compete with the CPC for the TPP ions. Indeed, though at the lowest parent PAH solution concentration the PAH yield was more than 10% lower in the presence of CPC (which was an observable inhibitory effect), at the highest parent PAH solution concentration this CPC addition had no discernable impact on the PAH yield (Fig. 3b). Besides the variations in the relative concentrations of CPC and PAH, this trend might also reflect the CPC/TPP binding likely being stronger at lower ionic strengths [30, 48].

Also measured was the impact of CPC addition on the PAH concentration within the coacervate phase. When the coacervates were prepared at the highest, 10 wt% (1.2 M) parent PAH solution concentration, CPC addition had very little effect on the coacervate PAH content (Fig. 3c). When the parent PAH concentration was reduced at a constant initial CPC concentration (and constant TPP:PAH molar ratio), however, the CPC addition effect became much more pronounced. While in the absence of CPC the coacervate PAH content remained constant with the parent PAH solution concentration, PAH concentration in coacervates formed in the presence of 25 mM CPC dropped from roughly 46 to 37 wt% as the PAH concentration was reduced by a factor of four (Fig. 3d). This change likely, again, reflected the fact that, at lower PAH concentrations, CPC can

https://doi.org/10.1016/j.colsurfa.2021.127490

more effectively compete with the PAH for the crosslinking TPP ions and (by inhibiting PAH/TPP association) reduce the ionic network density. Overall, these findings (i.e., high PAH yields and incremental reductions in the coacervate PAH contents) suggest that, though the presence of CPC may hinder coacervation, this hindrance plays a relatively minor role.

3.3. CPC Uptake Analysis

The CPC encapsulation expectedly increased with the initial CPC concentrations in the parent PAH and TPP solutions. As the CPC concentration in the parent TPP solution was raised from 28 to 140 mM (which elevated the overall CPC concentration in the final PAH/TPP/CPC mixture from 14 to 71 mM), the LC values increased from roughly 6 to 40 mg/g (red circles in Fig. 4a). Similarly, when the CPC was initially added to the parent PAH solutions, the LCs increased from 3 to 34 mg/g with similar added CPC amounts (black squares in Fig. 4a). Notably, incorporating CPC in TPP solutions prior to the PAH/TPP mixing generally resulted in higher LCs, likely because the initial CPC/TPP association helped to entrap CPC in the coacervate matrix. Indeed, while the LCs achieved by adding CPC to the TPP solutions were consistently higher than the overall CPC contents in the two-phase PAH/TPP/CPC mixtures (indicated by the dashed line in Fig. 4a), such preferential CPC uptake was only achieved at the highest CPC concentration when the CPC was initially added to the PAH solution. This CPC/TPP association requirement for concentrating CPC within the coacervate phase might stem from most of the coacervate volume being occupied by PAH and TPP, which (in the absence of considerable CPC/TPP affinity) likely hinders CPC uptake into the coacervate phase.

https://doi.org/10.1016/j.colsurfa.2021.127490

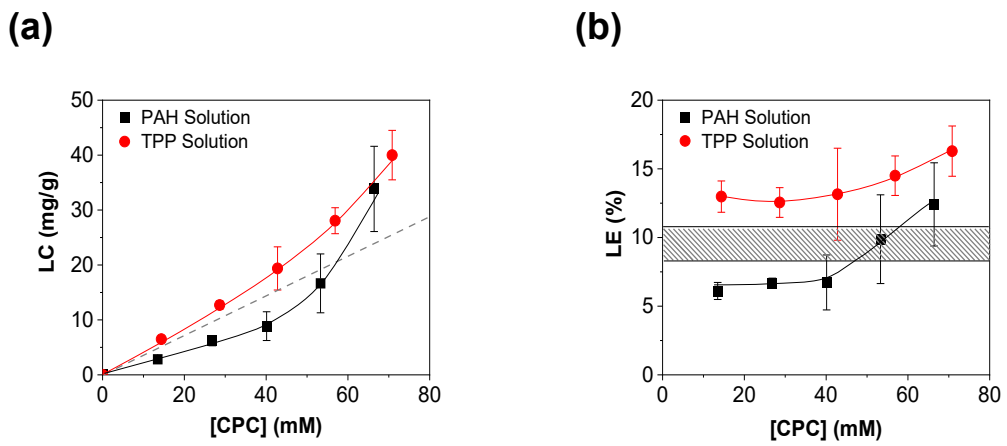

Fig. 4. CPC concentration effects on the (a) LC and (b) LE of CPC uptake into coacervates prepared from 10 wt% (1.2 M) PAH and 7.5 wt% (220 mM) TPP where the CPC was initially introduced into either the parent TPP solution or the parent PAH solution. The CPC concentrations indicated on the abscissa are those achieved upon the mixing of the parent PAH and TPP solutions. All data are mean ± SD, while the solid lines are guides to the eye. The dashed line in (a) shows the overall CPC content in the two-phase PAH/TPP/CPC mixtures, and approximates the LCs expected with uniform CPC partitioning between the coacervate and supernatant phases. Similarly, the shaded region in (b) indicates the range of percentages of the mixture weights made up by the coacervate phases, which approximates the range of LEs expected with uniform CPC partitioning.

Though CPC could be encapsulated in a range of different loadings, the LE values remained fairly low (between 6 and 16%). These LE values can be understood based on the low volume fraction occupied by the coacervate phases, which accounted for only ~8 – 11% of the mixture mass (see the shaded region in Fig. 4b). Since, at the compositions examined in this experiment, CPC was not strongly concentrated in the coacervates (see Fig. 4a), LEs comparable to the coacervate weight fractions were expected. Thus, the LE was 6 – 12% when the CPC was initially added to the PAH solution and 13 – 16% (Fig. 4b) when the CPC was initially added to the parent TPP solution (which resulted in more efficient encapsulation). Irrespective of these encapsulation methods, the LE modestly increased at higher CPC concentrations, possibly due to a rise in CPC/TPP association (which was expected due to the cooperativity of surfactant binding to multi- and polyvalent molecules of opposite charge [30, 56]). This increase in LE was also

https://doi.org/10.1016/j.colsurfa.2021.127490

qualitatively consistent with the earlier report on anionic surfactant (i.e., ibuprofen) encapsulation, where (albeit at different PAH/TPP concentrations) a highly pronounced increase in LE at higher surfactant concentrations also occurred [30].

The encapsulation properties also depended on the parent PAH solution concentration, which was varied at a fixed, 0.2:1 TPP:PAH molar ratio while initially dissolving matching amounts of CPC in both of the parent PAH/TPP solutions. Here, the LCs generally decreased with the PAH concentration, with (though the trend was nonmonotonic at the highest CPC concentration) the best LCs predominantly occurring at higher CPC and lower PAH contents (Fig. 5a). The lower-PAH compositions also corresponded to the highest achieved LE values, which reached the 20% range (black squares and red circles in Fig. 5b). The variations in LEs, however, did not show a clear monotonic trend.

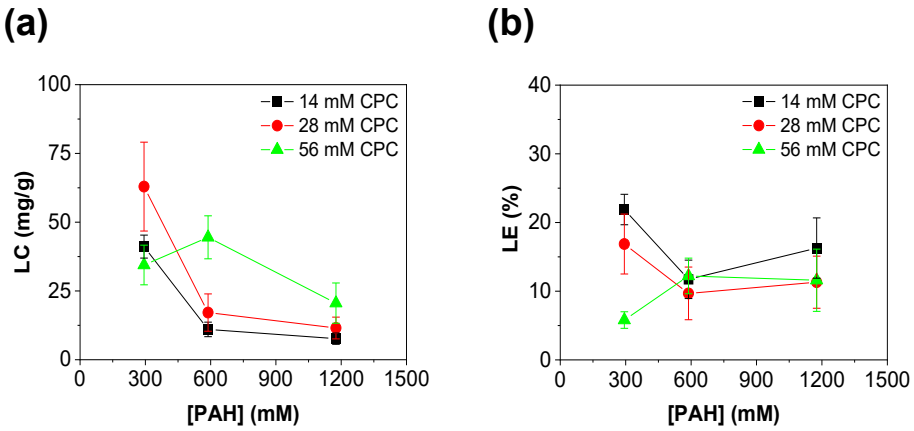

Fig. 5. Effect of PAH concentration on the (a) LC and (b) LE values. The three data sets correspond to three different (14 – 56 mM) overall CPC concentrations in the final PAH/TPP/CPC mixtures (which were achieved by adding matching CPC amounts in the parent PAH/TPP solutions). The TPP:PAH molar ratio was fixed at 0.20:1. All data are mean ± SD, while the lines are guides to the eye.

The higher LCs that were generally achieved at lower PAH concentrations were qualitatively consistent with those obtained upon the encapsulation of anionic, PAH-binding

https://doi.org/10.1016/j.colsurfa.2021.127490

payloads within PAH/TPP coacervates [22, 30]. This similarity likely reflected CPC/TPP binding (which acted analogously to the PAH/anionic surfactant binding) and the dilution of the encapsulated CPC at higher PAH concentrations due to a greater coacervate volume being formed [22, 30]. Conversely, the lack of a clear monotonic trend in some of this CPC encapsulation data might have stemmed from the LE being determined by a balance between two effects: (1) higher PAH concentrations generating a greater amount of coacervate, which enhanced CPC entrapment [22]; and (2) higher PAH/TPP concentrations reducing the uptake-enhancing CPC/TPP affinity [30]. Here, the drop in uptake affinity could either have arisen from the reduction in the CPC:TPP ratio (which lowered the likelihood of cooperative hydrophobic interactions between TPP-bound CPC molecules [30, 56]) or the higher ionic strengths [30, 48].

Regardless of the mechanisms underlying the above uptake trends, Figs. 4 and 5 suggested that the highest CPC loadings were generally achieved when: (1) the CPC was initially introduced into the parent TPP solution; (2) the CPC concentration was high; and (3) the overall PAH/TPP concentration in the phase-separating PAH/TPP/CPC mixture was low. All three of these observations were similar to those made previously on the encapsulation of anionic surfactant (ibuprofen) in PAH/TPP complexes, where extremely high (~30 wt%) ibuprofen loadings were achieved at even lower PAH concentrations via the method described in the Introduction [30]. To explore whether a similar effect could also be achieved with cationic surfactant (e.g., CPC) encapsulation, CPC/TPP colloidal dispersions (containing 28 – 84 mM CPC and 25 mM TPP) were prepared, whereupon small charges of 10 wt% (1.2 M) PAH solution were immediately added (in a 1:9 volume ratio) to form coacervates at the same 0.2:1 TPP:PAH molar ratio used in the other experiments (see Supplementary Data, Section A). Although the PAH and TPP concentrations in the final PAH/TPP/CPC mixtures were roughly 1.2 – 4.8× smaller than those

https://doi.org/10.1016/j.colsurfa.2021.127490

used to produce the coacervates described in Figs. 4 and 5, the CPC in these mixtures was initially concentrated around the TPP. Thus, despite the low PAH/TPP/CPC mixture volume fraction occupied by the coacervate phase (see Supplementary Data, Fig. S1) — and consistent with the previous findings on this type of encapsulation of ibuprofen [30] — the CPC was encapsulated in very large amounts, with LCs ranging from roughly 60 to 230 mg/g and LEs remaining in the 11 – 17% range (Fig. 6). In other words, just like in the case of the PAH-binding anionic surfactants [30], very high loadings (exceeding at least 20 wt%) can be achieved with cationic surfactants such as CPC.

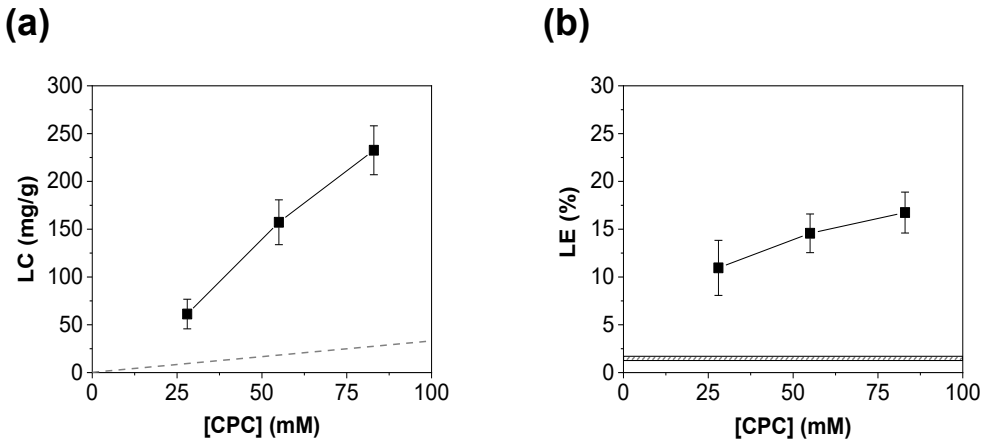

Fig. 6. CPC concentration effects on the (a) LC and (b) LE of CPC-bearing coacervates prepared by adding PAH (to generate a 0.2:1 TPP:PAH molar ratio) to colloidal CPC/TPP dispersions containing 28 – 84 mM CPC in 0.9 wt% (25 mM) TPP. The CPC concentrations are those achieved upon the addition of PAH. All data are mean ± SD, while the lines are guides to the eye. The dotted line in (a) shows the overall CPC content in the two-phase PAH/TPP/CPC mixtures, and approximates the LCs expected with uniform CPC partitioning between the coacervate and supernatant phases. Similarly, the shaded region in (b) indicates the range of percentages of the mixture weights made up by the coacervate phases, which approximates the range of LEs expected with uniform CPC partitioning.

3.4. Coacervate Swelling

Although there was no visible increase in the PAH/TPP coacervate weights upon their month-long storage in the presence of their supernatant phases (data are not shown), more

https://doi.org/10.1016/j.colsurfa.2021.127490

substantial swelling occurred when the coacervates were stored in tap water (see Fig. 7). The wet weights of CPC-free PAH/TPP coacervates stored in tap water increased by roughly 45% after one month (Fig. 7a and d). Afterward, however, this swelling plateaued (Fig. 7aiii, aiv, and d). This increased swelling upon placement into tap water, which likely reflected an increased osmotic pressure difference between the coacervate and supernatant phases, was qualitatively consistent with that measured previously for PAH/TPP coacervates [29] and those reported for polyelectrolyte complex coacervates (formed between oppositely charged polyelectrolyte molecules) in salt-free water [57, 58].

https://doi.org/10.1016/j.colsurfa.2021.127490

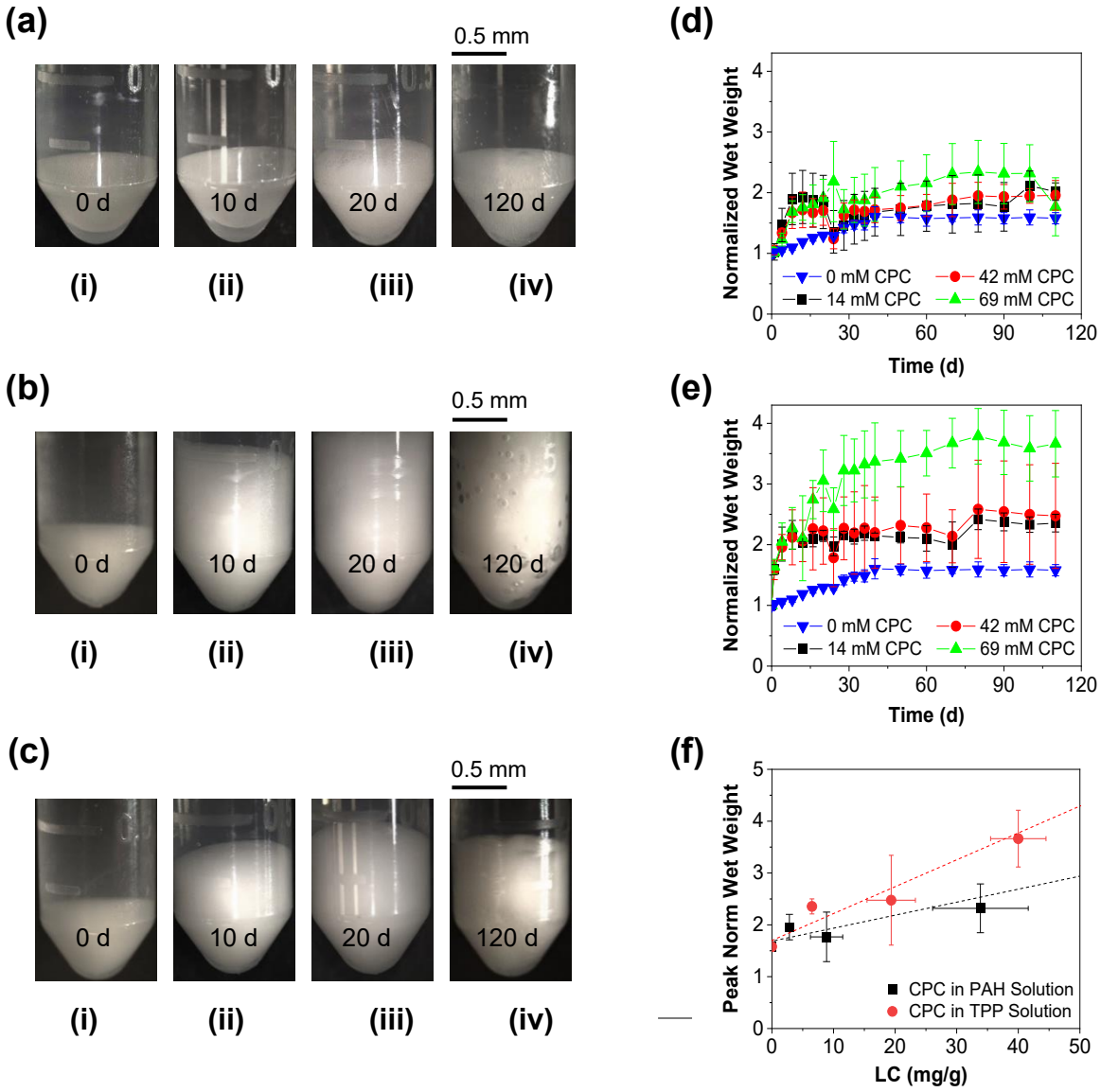

Fig. 7. Photographs of PAH/TPP coacervates prepared with (a) no CPC, (b) CPC added to the parent PAH solution, and (c) CPC added to the parent TPP solution after (i) 0, (ii) 10, (iii) 20 and (iv) 120 d of contact with room-temperature tap water (pH 9.6 ± 0.5 and turbidity ≈ 0.2 – 0.4 NTU); (d, e) gravimetric data on PAH/TPP coacervates where CPC was initially added to either to the (d) parent PAH solution or (e) parent TPP solution resulting in 0 – 69 mM final CPC concentrations in the PAH/TPP/CPC mixtures; and (f) peak swelling as a function of LC for coacervates where CPC was initially added to either the parent PAH solution or the parent TPP solution. All coacervates were prepared using 10 wt% (1.2 M) parent PAH solutions and 7.5 wt% (220 mM) parent TPP solutions. The final PAH/TPP/CPC mixtures used to form the coacervates in (b, c) both contained 69 ± 2 mM CPC. All data are mean ± SD, while the lines are guides to the eye.

https://doi.org/10.1016/j.colsurfa.2021.127490

The coacervate swelling generally increased with their CPC content (Fig. 7a – e). Moreover, coacervates where CPC was initially introduced into the parent TPP solution swelled more than those where the CPC was first dissolved in the parent PAH solution (Fig. 7d and e). At the highest, 69 mM CPC concentration, for instance, coacervates where the CPC was first added to the parent PAH solution swelled by more than twofold, while the coacervates where CPC was initially added to the parent TPP solution underwent more than threefold swelling. This strong, preparation method-dependent swelling indicated that: (1) despite its limited impact on the initial coacervate yield and PAH concentration (see Fig. 3), competitive CPC/TPP complexation affects PAH/TPP association; and (2) since the preparation dependence appeared to persist even after correcting for differences in LC (compare peak swelling versus LC curves in Fig. 7f), nonequilibrium aspects of competitive CPC/TPP and CPC/PAH association during coacervate preparation may have long-term implications on the coacervate performance. Further, despite the very substantial swelling of the CPC-loaded coacervates, they appeared to maintain their low solute permeabilities — i.e., upon their 10-d exposure to a solution of non-binding Rhodamine B dye (which was added to the tap water to check whether it would diffuse into the coacervate), there was no visible dye penetration into the coacervate networks (Supplementary Data, Section B).

The swelling of CPC-bearing coacervates was also sensitive to the presence of salts. This dependence was explored using 10 mM NaCl, $CaCl_2$, and Na_2SO_4 solutions, which served as extreme-case models of high tap water salinity/hardness [59, 60]. Simple electrolytes such as those used in this experiment are well known to inhibit coacervate formation, with multivalent salts (e.g., Na_2SO_4 and $CaCl_2$) producing a stronger inhibitory effect [9, 61]. The three salt types, however, produced highly disparate coacervate swelling. The NaCl solution increased swelling (diamonds in Fig. 8), possibly because of the competitive association of monovalent ions with crosslink-

https://doi.org/10.1016/j.colsurfa.2021.127490

forming ionic groups [62, 63], which may have weakened both CPC/TPP and PAH/TPP binding and, thus, decreased the intermolecular association within the coacervates [21]. This increased swelling was significantly more pronounced when the coacervates were stored in $CaCl_2$ solution (triangles in Fig. 8), reflecting the strong Ca^{2+} binding to the TPP [64, 65], which reduced the TPP crosslinking of the PAH. Another (albeit smaller) contribution to this $CaCl_2$ effect may have been that the concentration of the Cl^- ions in this solution, which could competitively associate with the PAH and CPC, was twice as high as in the case of NaCl. Conversely, when CPC-bearing coacervates were exposed to Na_2SO_4 solution, they swelled the least (circles in Fig. 8), even less than the CPC-bearing coacervates stored in tap water and, initially (until the swelling medium was replaced after the first day of the experiment), made the medium turbid. This diminished swelling may have been caused by the SO_4^{2-} ions — despite competing with the TPP for the PAH amine groups — forming insoluble complexes with the PAH (Supplementary Data, Section C). Thus, PAH/SO_4^{2-} complexation reduced PAH/TPP coacervate swelling and gave rise to initial turbidity by precipitating the uncomplexed PAH.

https://doi.org/10.1016/j.colsurfa.2021.127490

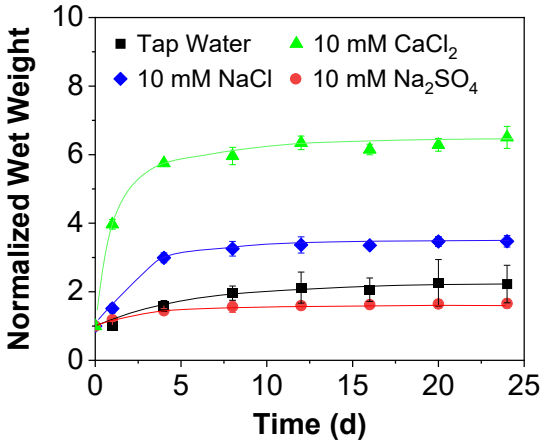

Fig. 8. CPC-loaded PAH/TPP coacervate swelling in various aqueous release/swelling media photographed after (a) 0, (b) 2, (c) 4 and (d) 10 d of equilibration, and (e) normalized coacervate wet weights as functions of time. The release/swelling media were tap water (pH 9.6 ± 0.5 and turbidity ≈ 0.2 – 0.4 NTU) and 10 mM NaCl, $CaCl_2$, and Na_2SO_4 solutions. All coacervates were prepared by using 42 mM final CPC concentration in the PAH/TPP/CPC mixtures, where CPC was dissolved in 10 wt% (1.2 M) PAH and mixed with 7.5 wt% (220 mM) blank TPP solutions. All data are mean ± SD, while the lines are guides to the eye.

Interestingly, though the ionic strengths of all swelling media used in this study were lower than that of the phosphate-buffered saline (PBS) used in some of the prior experiments on the PAH/TPP coacervates [22, 30], the swelling of the CPC-loaded coacervates was generally greater than that seen in that work. This difference may have reflected a possible disruption of the coacervate networks by the CPC which, from visual observation (see inset in Fig. 3a), produced a greater change in the coacervate properties than, for instance, that produced by the weak anionic surfactant, ibuprofen [30]. Alternatively, the phosphate ions in PBS (which can also form coacervates with PAH [19, 23, 27]) may have diminished swelling like the SO_4^{2-} ions in the present work. Though understanding these swelling effects requires further study, it is clear that the PAH/TPP coacervate swelling can be highly sensitive to both the payloads they carry and their swelling media.

https://doi.org/10.1016/j.colsurfa.2021.127490

3.5. CPC Uptake Effect on Coacervate Spreading

Because the PAH/TPP coacervates were, strictly, complex fluids rather than true gels, they ultimately flowed when left over extended times without solid enclosures (e.g., microcentrifuge tubes). As shown in Fig. 9, while coacervates prepared from parent PAH solutions containing 2.5 – 10 wt% (0.29 – 1.2 M) PAH and either 0 or 56 mM CPC initially occupied almost identical areas, they spread over time in a composition-dependent manner. CPC-free coacervates prepared at higher PAH concentrations flowed the most — likely due to the elevated ionic strengths generated by the release of monovalent counterions upon PAH/TPP complexation — while those loaded with CPC spread the least (with a less than 25% increase in diameter) and were insensitive to the parent solution PAH concentration. This diminished spreading suggested that strong surfactant encapsulation can stabilize the PAH/TPP coacervates against spreading, possibly by forming surfactant/TPP (or surfactant/PAH [30]) complexes with longer relaxation times, or through a possible thickening effect created by encapsulated surfactant micelles. This reduced flowability was also evident upon manual molding of the coacervates. Further impacts on spreading rates might also stem from surfactant effects on the surface energies of the application surface/water, application surface/coacervate, and coacervate/water interfaces, which (though all coacervates appeared to spread spontaneously) may have affected the thermodynamic driving force for coacervate spreading [66]. Regardless of its underlying causes, this diminished spreading could help keep the CPC-loaded PAH/TPP coacervates at their application sites and may, at least in part, explain their weakened adhesion to the microcentrifuge tubes (see Section 3.2).

https://doi.org/10.1016/j.colsurfa.2021.127490

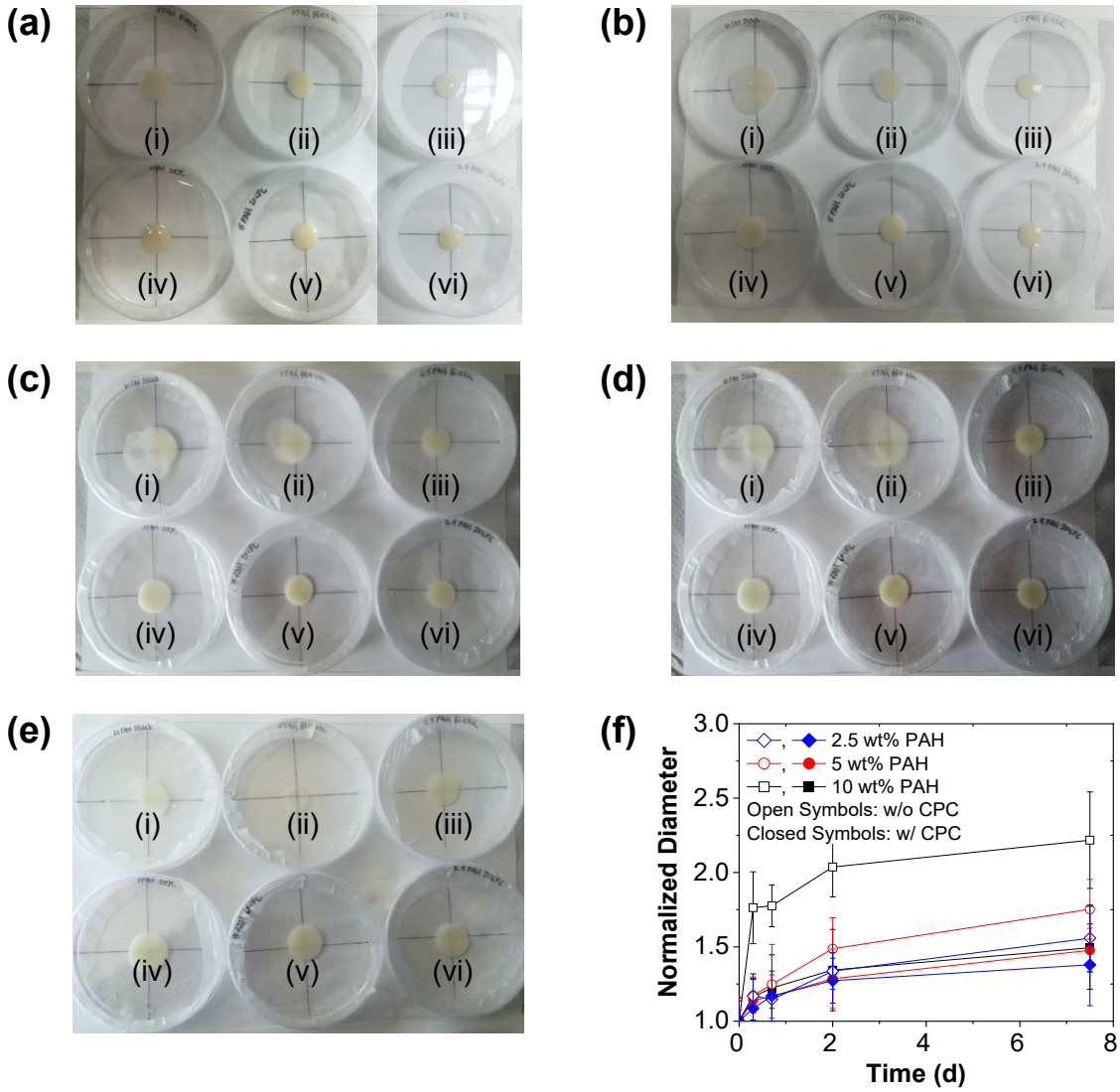

Fig. 9. Effects of parent PAH solution concentration and CPC uptake on the spreading behavior of PAH/TPP coacervates when stored in their supernatant solutions photographed after (a) 0.0, (b) 0.3, (c) 0.7, (d) 2.0, and (e) 7.5 d of equilibration, and (f) changes in the normalized coacervate diameters in images (a – e). The six coacervate samples are (i) 10 wt% (1.2 M) PAH without CPC, (ii) 5 wt% (0.59 M) PAH without CPC, (iii) 2.5 wt% (0.29 M) PAH without CPC, (iv) 10 wt% (1.2 M) PAH with CPC, (v) 5 wt% (0.59 M) PAH with CPC and (vi) 2.5 wt% (0.29 M) PAH with CPC. In each CPC-bearing coacervate, the CPC was loaded by introducing 56 mM CPC into both of the parent PAH and TPP solutions. All quantitative data are mean ± SD, while the lines are guides to the eye.

https://doi.org/10.1016/j.colsurfa.2021.127490

3.6. CPC Release Analysis

When placed in tap water, all tested PAH/TPP coacervates slowly released CPC over multi-month timescales, with no more than 10 – 15% of their payloads released after 5 – 7 months (Fig. 10a). When the release profiles were plotted in terms of the percentage of CPC released, the fractional release was fastest when the initial CPC content was lower (Fig. 10a). When the same data were replotted in terms of the total mass of CPC released, however, this situation generally became reversed, with the coacervates bearing the most CPC generally exhibiting the highest release rates (Fig. 10b). These trends and multi-month release times were qualitatively consistent with those reported previously for other binding payloads, namely ibuprofen [30] and the anionic dye Fast Green FCF [22]. A notable difference with much of the data in these prior reports, however, was the relative insensitivity of the total payload mass released to the CPC content within the coacervates (Fig. 10b). This feature was especially apparent when the variable burst releases from the first day of the experiment were subtracted from the release profiles, whereupon the release curves largely overlapped (Fig. 10c). In each case, the release rate was typically fastest at the beginning (in the roughly 1 – 10 μg/d range) and then decreased with time, dropping below 1 μg/d after 1 – 2 weeks (Fig. 10d). Nonetheless, slow CPC release (at rates exceeding 0.1 μg/d) persisted over several months. These trends occurred regardless of whether the CPC was initially introduced into the parent PAH solution (Fig. 10a – d) or parent TPP solution (Fig. 10e – h), though when CPC was initially added to the parent TPP solution, release rates near or above 1 μg/d tended to persist longer (i.e., for approximately 1 month; see Fig. 10h).

https://doi.org/10.1016/j.colsurfa.2021.127490

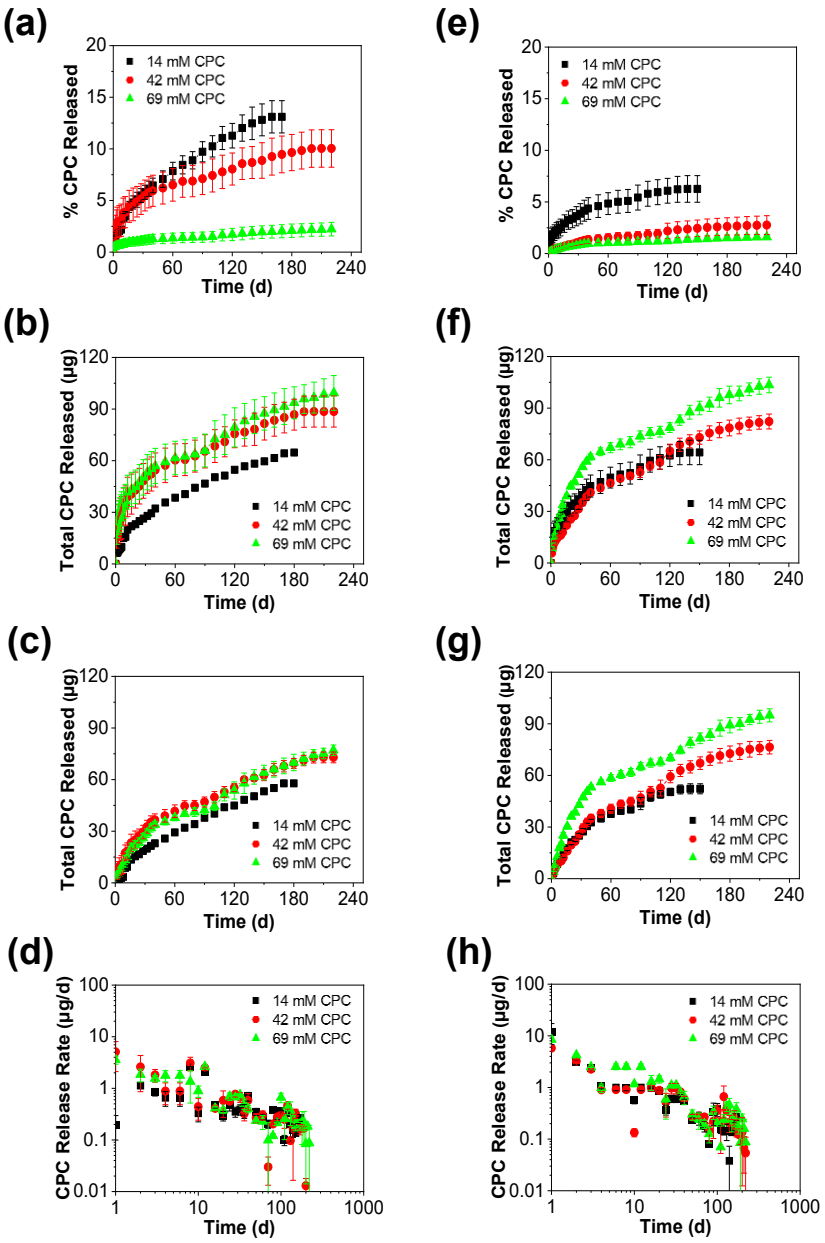

Fig. 10. CPC release into pH 9.6 ± 0.5 and turbidity ≈ 0.2 – 0.4 NTU tap water from coacervates prepared by initially adding the CPC to (a – d) the 10 wt% (1.2 M) parent PAH solution or (e – h) the 7.5 wt% (220 mM) parent TPP solution. The release profiles show the (a, e) percent of the encapsulated CPC released, (b, f) mass of CPC released, (c, g) mass of CPC released after the initial burst release (i.e., after the initial day of the release experiment) and (d, h) CPC release rate as functions of time. The overall CPC concentration in the PAH/TPP/CPC mixtures from which the coacervates were formed (shown by the three data sets in each plot) was either 14 mM, 42 mM, or 69 mM. All data are mean ± SD, while the lines are guides to the eye.

https://doi.org/10.1016/j.colsurfa.2021.127490

The long-term CPC release, as discussed in prior reports [22, 30], likely reflected the low solute permeability of the PAH/TPP coacervates. Likewise, the reduction in the CPC release rate with time was probably (at least in part) caused by the increased diffusion path lengths [22, 30]. Other possible effects that may have affected these release rates include temporal changes in the coacervate swelling, porosity, and association with CPC (all of which might have altered the coacervate solute permeability [22]). Another interesting feature of the release profiles (i.e., profiles showing the masses of CPC released as functions of time) was their relative insensitivity to the LC values, which (as shown in Fig. 4a) monotonically increased with the CPC concentration in the parent PAH and TPP solutions. This insensitivity might have, again, reflected the reversible and cooperative association of the encapsulated CPC molecules, either with other CPC molecules or with the TPP. Such binding interactions generally reduce diffusion rates [67] and, when cooperative, may be more prevalent at higher payload concentrations [22].

Given the likely CPC affinity for the coacervate, it was also possible that sink conditions in the release media were not readily achieved (i.e., that the driving force for the release was reduced by CPC accumulation in the release media). To explore this possibility, one of the release experiments was repeated using a tenfold larger release medium volume (Supplementary Data, Fig. S4). This experiment revealed a severalfold increase in initial release rates. After a few days, however, the difference between these release rates decreased (see Fig. S4c). Although the release rates with the greater release medium volume remained generally higher throughout this 21-d experiment, they were on the same order of magnitude as those with the lower release medium volume. Thus, though sink conditions were not strictly achieved when the strongly surface-active CPC was released from the coacervates, the relatively modest differences in release rates in Fig. S4 suggested that the multi-month CPC release would persist irrespective of the release volume.

https://doi.org/10.1016/j.colsurfa.2021.127490

3.7. Further Discussion

Collectively, the very slow CPC release rates obtained in this study confirm that, like the previously studied anionic surfactant (ibuprofen) [30], cationic surfactants can be released from PAH/TPP coacervates over multi-month timescales. The insensitivity of these release rates to the LC, however, suggests that the use of PAH/TPP coacervates for CPC-release-mediated disinfection should be limited to applications where the release media has low volumes and is not rapidly exchanged (as otherwise, the CPC concentrations accumulated in the release media may be too low to be efficacious). This constraint stems from the CPC release rates (~1 μg/d over the first several weeks) being relatively low compared to its minimal inhibitory concentrations (MICs) for common bacteria, many of which fall in the high 0.5 – 4 μg/mL range [68-71]. Though these release rates can likely be adjusted by varying the coacervate/release medium interfacial areas, the CPC amounts they release in Fig. 10 enables only ~1 mL/d of freshly supplied water to reach the MIC. To achieve antibacterial activity in a broader range of conditions, however, the PAH/TPP coacervates can likely be combined with more potent bactericides, which can be effective at much lower concentrations, or bactericidal molecules that can be released more quickly [29]. Likewise, the surfactant release demonstrated herein could have other potential applications, such as surface tension control/enhancement of wetting properties.

Besides these sustained release application-oriented considerations, this study provides several new physicochemical insights on the properties of PAH/TPP (and other polyamine/multivalent anion) coacervates. First, it demonstrates that like the ionic polymers (e.g., PAH), small multivalent ions such as TPP can (through ionic association) concentrate oppositely charged surfactants within coacervates. Thus, the high (> 20 wt%) LCs reached in this work challenge the previously held view that effective solute encapsulation in polyamine/multivalent

https://doi.org/10.1016/j.colsurfa.2021.127490

anion coacervates requires the payload to bear a net negative charge [8], and show that — as long as the payload binds to the multivalent anion — this negative charge requirement can be circumvented. Second, this study reveals how the mixing order affects the PAH/TPP coacervate encapsulation properties. By demonstrating that mixing the payload with the oppositely charged coacervate component (TPP in this work) first enhances encapsulation efficiency (which parallels recent findings on protein encapsulation in polyanion/polycation coacervates [72]), our results support the view that encapsulation within complex coacervates tends to be kinetically (rather than thermodynamically) controlled. Third, the mixing order-dependent swelling of the CPC-loaded PAH/TPP coacervates (which persists even for coacervates with similar CPC contents) indicates that — contrary to the frequent treatment of coacervates as equilibrium phases [73, 74] — their long-term properties can reflect nonequilibrium effects.

Additionally, this study reveals that, when placed into multivalent salt solutions, polyelectrolyte/multivalent counterion coacervate swelling can be highly ion-specific, with ambient ions that bind the coacervate-forming small ions increasing the swelling and those that form insoluble complexes with the polyelectrolyte decreasing the swelling. Lastly, by demonstrating that surfactant uptake can reduce PAH/TPP coacervate spreading from their application sites, this study points to the possible use of surfactants in these (and other polyelectrolyte/multivalent counterion) coacervates as rheological modifiers. These insights establish more thorough guidelines for the design and use of PAH/TPP coacervates and provide a basis for further fundamental work (e.g., on the origins of the mixing order-dependent swelling properties or on the molecular and microstructural effects underlying the surfactant-induced changes in their flow/spreading characteristics).

https://doi.org/10.1016/j.colsurfa.2021.127490

4. CONCLUSIONS

Using CPC as a model molecule, we have shown that — like their anionic counterparts [30] — cationic surfactants can be encapsulated in PAH/TPP coacervates (with LCs exceeding 20 wt%) and released over multiple-month timescales. The encapsulation properties are improved by initially introducing the surfactant into the parent TPP solution (rather than the parent PAH solution) which, by binding the cationic surfactant, concentrates it near the PAH and TPP during the coacervation process. The highest LCs are achieved through this approach by generating PAH/TPP/CPC mixtures with high surfactant concentrations and low PAH/TPP concentrations. This CPC uptake reveals that high amounts of small molecule payload can be encapsulated within polyamine/small multivalent anion coacervates without requiring payload affinity for the polymer, thus (in cases where the payload species associate with the small multivalent anion) extending the use of these coacervates to the effective encapsulation of cationic actives.

Once encapsulated, the cationic surfactant strongly increases the PAH/TPP coacervate swelling in water (especially when coacervates are prepared by first adding the CPC into the TPP solution) but decreases its spreading from its application site. Thus, cationic surfactant/TPP binding appears to strongly affect PAH/TPP coacervate properties. Since the magnitude of this effect depends on the mixing method by which CPC is loaded into the coacervate (even when the overall coacervate CPC content is held constant), these analyses show that even the long-term properties of macroscopic complex coacervates — which are often treated as equilibrium phases — can be governed by nonequilibrium effects.

Regardless of the CPC content of the coacervates, its release rates diminish significantly with time and, when expressed in terms of the percent of the payload released, depend strongly on the CPC amount initially present in the coacervate (i.e., the LC). When expressed as a total

https://doi.org/10.1016/j.colsurfa.2021.127490

surfactant mass released, however, the release profiles become relatively weak functions of the LC and of whether the CPC was initially introduced in the parent PAH or the parent TPP solution (though the initial drop in the release rate appears to be slower when the CPC is initially introduced into the TPP solution). Taken together, these findings suggest the possibility of using PAH/TPP coacervates for the low-dose sustained release of cationic surfactants in diverse applications, such as surface cleaning and disinfection, and enhancement of wetting properties.

Declaration of Competing Interest. YL declares a financial interest in a patent (US 9814778 B2) on the use of PAH/TPP coacervates as adhesives and sustained release vehicles. Aside from this patent, the authors declare that they have no known competing financial interests or personal relationships that could have appeared to influence the work reported in this paper.

Acknowledgments. The authors gratefully acknowledge the National Science Foundation (IIP-1701104) for the financial support of this work, and Kunal Choudhuri (Univ. of Toledo) for assistance with UV-vis spectroscopy.

REFERENCES:

[1] E. Spruijt, A.H. Westphal, J.W. Borst, M.A. Cohen Stuart, J. van der Gucht, Binodal compositions of polyelectrolyte complexes, Macromolecules 43(15) (2010) 6476-6484.

[2] F. Tiebackx, Gleichzeitige ausflockung zweier kolloide, Zeitschr. f. Chem. und Ind. der Kolloide 8(4) (1911) 198-201.

[3] Q. Wang, J.B. Schlenoff, The polyelectrolyte complex/coacervate continuum, Macromolecules 47(9) (2014) 3108-3116.

[4] C.G. De Kruif, F. Weinbreck, R. de Vries, Complex coacervation of proteins and anionic polysaccharides, Curr. Opin. Colloid Interface Sci. 9(5) (2004) 340-349.

[5] S. Jacksch, D. Kaiser, S. Weis, M. Weide, S. Ratering, S. Schnell, M. Egert, Influence of Sampling Site and other Environmental Factors on the Bacterial Community Composition of Domestic Washing Machines, Microorganisms 8(1) (2020) 30.

[6] Y. Wang, K. Kimura, Q. Huang, P.L. Dubin, W. Jaeger, Effects of salt on polyelectrolyte−micelle coacervation, Macromolecules 32(21) (1999) 7128-7134.

https://doi.org/10.1016/j.colsurfa.2021.127490

[7] D. Li, M.S. Kelkar, N.J. Wagner, Phase behavior and molecular thermodynamics of coacervation in oppositely charged polyelectrolyte/surfactant systems: a cationic polymer JR 400 and anionic surfactant SDS mixture, Langmuir 28(28) (2012) 10348-10362.

[8] H.G. Bagaria, M.S. Wong, Polyamine–salt aggregate assembly of capsules as responsive drug delivery vehicles, J. Mater. Chem. 21(26) (2011) 9454-9466.

[9] H. Bungenberg de Jong, Complex colloid systems, Colloid Science 2 (1949) 335-432.

[10] A. Momeni, M.J. Filiaggi, Rheology of polyphosphate coacervates, J. Rheol. 60(1) (2016) 25-34.

[11] N.R. Johnson, Y. Wang, Coacervate delivery systems for proteins and small molecule drugs, Taylor & Francis, 2014.

[12] B.D. Winslow, H. Shao, R.J. Stewart, P.A. Tresco, Biocompatibility of adhesive complex coacervates modeled after the sandcastle glue of Phragmatopoma californica for craniofacial reconstruction, Biomaterials 31(36) (2010) 9373-9381.

[13] C. Schmitt, S.L. Turgeon, Protein/polysaccharide complexes and coacervates in food systems, Adv. Colloid Interface Sci. 167(1-2) (2011) 63-70.

[14] R.Y. Lochhead, L.R. Huisinga, T. Waller, Deposition from conditioning shampoo: Optimizing coacervate formation, Cosmetics and Toiletries 121(3) (2006) 75-82.

[15] L.A. Bosnea, T. Moschakis, C.G. Biliaderis, Complex coacervation as a novel microencapsulation technique to improve viability of probiotics under different stresses, Food Bioproc. Tech. 7(10) (2014) 2767-2781.

[16] Z. Xiao, W. Liu, G. Zhu, R. Zhou, Y. Niu, Production and characterization of multinuclear microcapsules encapsulating lavender oil by complex coacervation, Flavour Fragr. J. 29(3) (2014) 166-172.

[17] M. Zhao, N.S. Zacharia, Sequestration of Methylene Blue into polyelectrolyte complex coacervates, Macromol. Rapid Commun. 37(15) (2016) 1249-1255.

[18] Y.f. Wang, J.Y. Gao, P.L. Dubin, Protein separation via polyelectrolyte coacervation: Selectivity and efficiency, Biotechnol. Progr. 12(3) (1996) 356-362.

[19] P. Andreozzi, C. Ricci, J.E.M. Porcel, P. Moretti, D. Di Silvio, H. Amenitsch, M.G. Ortore, S.E. Moya, Mechanistic study of the nucleation and conformational changes of polyamines in presence of phosphate ions, J. Colloid Interface Sci. 543 (2019) 335-342.

[20] S.E. Herrera, M.L. Agazzi, M.L. Cortez, W.A. Marmisollé, M. Tagliazucchi, O. Azzaroni, Polyamine Colloids Cross-Linked with Phosphate Ions: Towards Understanding the Solution Phase Behavior, ChemPhysChem 20(8) (2019) 1044-1053.

[21] P.G. Lawrence, Y. Lapitsky, Ionically cross-linked poly(allylamine) as a stimulus-responsive underwater adhesive: Ionic strength and pH effects, Langmuir 31(4) (2015) 1564-1574.

[22] P.G. Lawrence, P.S. Patil, N.D. Leipzig, Y. Lapitsky, Ionically cross-linked polymer networks for the multiple-month release of small molecules, ACS Appl. Mater. Interfaces 8(7) (2016) 4323-4335.

[23] W.A. Marmisollé, J. Irigoyen, D. Gregurec, S. Moya, O. Azzaroni, Supramolecular Surface Chemistry: Substrate-Independent, Phosphate-Driven Growth of Polyamine-Based Multifunctional Thin Films, Adv. Funct. Mater. 25(26) (2015) 4144-4152.

[24] V.S. Murthy, S.B. Kadali, M.S. Wong, Polyamine-guided synthesis of anisotropic, multicompartment microparticles, ACS Appl. Mater. Interfaces 1(3) (2009) 590-596.

[25] R.K. Rana, V.S. Murthy, J. Yu, M.S. Wong, Nanoparticle self-assembly of hierarchically ordered microcapsule structures, Adv. Mater. 17(9) (2005) 1145-1150.

[26] M.L. Agazzi, S.E. Herrera, M.L. Cortez, W.A. Marmisollé, C. von Bilderling, L.I. Pietrasanta, O. Azzaroni, Continuous assembly of supramolecular polyamine–phosphate networks on surfaces: preparation and permeability properties of nanofilms, Soft Matter 15(7) (2019) 1640-1650.

[27] J. Yu, V.S. Murthy, R.K. Rana, M.S. Wong, Synthesis of nanoparticle-assembled tin oxide/polymer microcapsules, Chem. Commun. (10) (2006) 1097-1099.

[28] Y. Huang, P.G. Lawrence, Y. Lapitsky, Self-assembly of stiff, adhesive and self-healing gels from common polyelectrolytes, Langmuir 30(26) (2014) 7771-7777.

[29] S.S. Alam, Y. Seo, Y. Lapitsky, Highly sustained release of bactericides from complexcoacervates, ACS Appl. Bio Mater. 3(12) (2020) 8427-8437.

[30] U.K. de Silva, J.L. Brown, Y. Lapitsky, Poly(allylamine)/tripolyphosphate coacervates enable high loading and multiple-month release of weakly amphiphilic anionic drugs: an in vitro study with ibuprofen, RSC Adv. 8(35) (2018) 19409-19419.

[31] T.R. Hoare, D.S. Kohane, Hydrogels in drug delivery: Progress and challenges, Polymer 49(8) (2008) 1993-2007.

[32] A. Ridell, H. Evertsson, S. Nilsson, L.O. Sundelöf, Amphiphilic association of ibuprofen and two nonionic cellulose derivatives in aqueous solution, J. Pharm. Sci. 88(11) (1999) 1175-1181.

[33] J. Sjöström, L. Piculell, Simple gel swelling experiments distinguish between associating and nonassociating polymer− surfactant pairs, Langmuir 17(13) (2001) 3836-3843.

[34] Y.I. González, M. Stjerndahl, D. Danino, E.W. Kaler, Spontaneous vesicle formation and phase behavior in mixtures of an anionic surfactant with imidazoline compounds, Langmuir 20(17) (2004) 7053-7063.

[35] C.M. Dvoracek, G. Sukhonosova, M.J. Benedik, J.C. Grunlan, Antimicrobial behavior of polyelectrolyte− surfactant thin film assemblies, Langmuir 25(17) (2009) 10322-10328.

[36] M.F. Jurczyk, D.T. Floyd, B.H. Grüning, Cationic Surfactants and Quaternary Derivatives for Hair and Skin Care, in: R. Schueller, P. Romanowski (Eds.), Conditioning Agents for Hair and Skin, Marcel Dekker, Inc, New York, 1999, pp. 223-250.

[37] D.S. Murphy, Fabric softener technology: A review, J. Surfactants Deterg. 18(2) (2015) 199-204.

[38] L. Abezgauz, K. Kuperkar, P.A. Hassan, O. Ramon, P. Bahadur, D. Danino, Effect of Hofmeister anions on micellization and micellar growth of the surfactant cetylpyridinium chloride, J. Colloid Interface Sci. 342(1) (2010) 83-92.

[39] N. Baker, A.J. Williams, A. Tropsha, S. Ekins, Repurposing quaternary ammonium compounds as potential treatments for COVID-19, Pharm. Res. 37 (2020) 1-4.

[40] D.L. Popkin, S. Zilka, M. Dimaano, H. Fujioka, C. Rackley, R. Salata, A. Griffith, P.K. Mukherjee, M.A. Ghannoum, F. Esper, Cetylpyridinium chloride (CPC) exhibits potent, rapid activity against influenza viruses in vitro and in vivo, Pathogens & Immunity 2(2) (2017) 253.

[41] D. Abouhussein, M.A. El Nabarawi, S.H. Shalaby, A. Abd El-Bary, Cetylpyridinium chloride chitosan blended mucoadhesive buccal films for treatment of pediatric oral diseases, J. Drug Del. Sci. Technol. (2020) 101676.

[42] J.-E. Lee, J.-M. Lee, Y. Lee, J.-W. Park, J.-Y. Suh, H.-S. Um, Y.-G. Kim, The antiplaque and bleeding control effects of a cetylpyridinium chloride and tranexamic acid mouth rinse in patients with gingivitis, J. Periodontal Implant Sci. 47(3) (2017) 134-142.

[43] F. Teng, T. He, S. Huang, C.-P. Bo, Z. Li, J.-L. Chang, J.-Q. Liu, D. Charbonneau, J. Xu, R. Li, Cetylpyridinium chloride mouth rinses alleviate experimental gingivitis by inhibiting dental plaque maturation, Int. J. Oral Sci. 8(3) (2016) 182-190.

[44] W. Brocks, H. Eberhardt, A. Kalbfleisch, K.-h. Kischka, T. Krause, E. Racky, Cosmetic or dermatological agent in the form of a creamy permanent mousse or a stable foamed cream, U.S. Patent Application 10/432,408 (2004).

[45] H. Van Dort, Sunscreens based on substituted hydrocarbyl functional siloxanes for household, health, and personal care applications, U.S. Patent Application 10/827,478 (2004).

[46] P. Zhu, G. Sun, Antimicrobial finishing of wool fabrics using quaternary ammonium salts, J. Appl. Polym. Sci. 93(3) (2004) 1037-1041.

[47] S. Prochazkova, K.M. Vårum, K. Ostgaard, Quantitative determination of chitosans by ninhydrin, Carbhydr. Polym. 38(2) (1999) 115-122.

[48] N. Jain, S. Trabelsi, S. Guillot, D. McLoughlin, D. Langevin, P. Letellier, M. Turmine, Critical aggregation concentration in mixed solutions of anionic polyelectrolytes and cationic surfactants, Langmuir 20(20) (2004) 8496-8503.

[49] M. Olvera de la Cruz, L. Belloni, M. Delsanti, J. Dalbiez, O. Spalla, M. Drifford, Precipitation of highly charged polyelectrolyte solutions in the presence of multivalent salts, J. Chem. Phys. 103(13) (1995) 5781-5791.

[50] A. Flilissa, P. Méléard, A. Darchen, Cetylpyridinium removal using phosphate-assisted electrocoagulation, electroreduction and adsorption on electrogenerated sorbents, Chem. Eng. J. 284 (2016) 823-830.

[51] J. Beukenkamp, W. Rieman, S. Lindenbaum, Behavior of condensed phosphates in anion-exchange chromatography, Anal. Chem. 26(3) (1954) 505-512.

[52] A.I. Petrov, A.A. Antipov, G.B. Sukhorukov, Base− acid equilibria in polyelectrolyte systems: From weak polyelectrolytes to interpolyelectrolyte complexes and multilayered polyelectrolyte shells, Macromolecules 36(26) (2003) 10079-10086.

[53] A. Katchalsky, P. Spitnik, Potentiometric titrations of polymethacrylic acid, J. Polym. Sci. 2(4) (1947) 432-446.

[54] V.A. Izumrudov, M.V. Zhiryakova, S.E. Kudaibergenov, Controllable stability of DNA-containing polyelectrolyte complexes in water–salt solutions, Biopolymers 52(2) (1999) 94-108.

[55] K.E. Richardson, Z. Xue, Y. Huang, Y. Seo, Y. Lapitsky, Physicochemical and antibacterial properties of surfactant mixtures with quaternized chitosan microgels, Carbohydr. Polym. 93(2) (2013) 709-717.

[56] K. Murakami, Complex formation between dodecylpyridinium chloride and multicharged anionic planar substances, Langmuir 20(19) (2004) 8183-8191.

[57] H.M. Fares, Q. Wang, M. Yang, J.B. Schlenoff, Swelling and inflation in polyelectrolyte complexes, Macromolecules 52(2) (2018) 610-619.

[58] F.G. Hamad, Q. Chen, R.H. Colby, Linear viscoelasticity and swelling of polyelectrolyte complex coacervates, Macromolecules 51(15) (2018) 5547-5555.

[59] B. Lanz, A. Provins, The demand for tap water quality: Survey evidence on water hardness and aesthetic quality, Water Resour. Econ. 16 (2016) 52-63.

[60] D. Pearson, S. Chakraborty, B. Duda, B. Li, D.C. Weindorf, S. Deb, E. Brevik, D. Ray, Water analysis via portable X-ray fluorescence spectrometry, J. Hydrol. 544 (2017) 172-179.

[61] S. Perry, Y. Li, D. Priftis, L. Leon, M. Tirrell, The effect of salt on the complex coacervation of vinyl polyelectrolytes, Polymers 6(6) (2014) 1756-1772.

[62] F. Horkay, I. Tasaki, P.J. Basser, Osmotic swelling of polyacrylate hydrogels in physiological salt solutions, Biomacromolecules 1(1) (2000) 84-90.

[63] A. Katchalsky, I. Michaeli, Polyelectrolyte gels in salt solutions, J. Polym. Sci. 15(79) (1955) 69-86.

[64] I. Greenwald, The effect of phosphate on the solubility of calcium carbonate and of bicarbonate on the solubility of calcium and magnesium phosphates, J. Biol. 161 (1945) 697-704.

[65] E. De Kort, M. Minor, T. Snoeren, T. Van Hooijdonk, E. Van Der Linden, Calcium-binding capacity of organic and inorganic ortho-and polyphosphates, Dairy Sci. Technol. 89(3-4) (2009) 283-299.

[66] G. Dardelle, P. Erni, Three-phase interactions and interfacial transport phenomena in coacervate/oil/water systems, Adv. Colloid Interface Sci. 206 (2014) 79-91.

[67] E.L. Cussler, Diffusion: Mass Transfer in Fluid Systems, Cambridge University Press2009.

[68] J.-Y. Fang, Y.-K. Lin, P.-W. Wang, A. Alalaiwe, Y.-C. Yang, S.-C. Yang, The droplet-size effect of squalene@ cetylpyridinium chloride nanoemulsions on antimicrobial potency against planktonic and biofilm MRSA, Int. J. Nanomedicine 14 (2019) 8133-8147.

[69] J. Hrenovic, T. Ivankovic, L. Sekovanic, M. Rozic, Toxicity of dodecylpyridinium and cetylpyridinium clorides against phosphate-accumulating bacterium, Open Life Sci. 3(2) (2008) 143-148.

[70] L. Irizarry, T. Merlin, J. Rupp, J. Griffith, Reduced susceptibility of methicillin-resistant Staphylococcus aureus to cetylpyridinium chloride and chlorhexidine, Chemotherapy 42(4) (1996) 248-252.

[71] T. Verspecht, E.R. Herrero, L. Khodaparast, L. Khodaparast, N. Boon, K. Bernaerts, M. Quirynen, W. Teughels, Development of antiseptic adaptation and cross-adapatation in selected oral pathogens in vitro, Sci. Rep. 9(1) (2019) 1-13.

[72] M. Zhao, N.S. Zacharia, Protein encapsulation via polyelectrolyte complex coacervation: Protection against protein denaturation, J. Chem. Phys. 149(16) (2018) 163326.

[73] A. Salehi, R.G. Larson, A molecular thermodynamic model of complexation in mixtures of oppositely charged polyelectrolytes with explicit account of charge association/dissociation, Macromolecules 49(24) (2016) 9706-9719.

[74] C.E. Sing, Development of the modern theory of polymeric complex coacervation, Adv. Colloid Interface Sci. 239 (2017) 2-16.